Acta Crystallographica Section D
Biological Crystallography
ISSN 0907-4449

SAD phasing by *OASIS*-2004: case studies of dual-space fragment extension

De-qiang Yao,[a,b,c]‡ Sheng Huang,[b]‡ Jia-wei Wang,[a]‡§ Yuan-xin Gu,[a] Chao-de Zheng,[a] Hai-fu Fan,[a]* Nobuhisa Watanabe[d] and Isao Tanaka[d]

[a]Beijing National Laboratory for Condensed Matter Physics, Institute of Physics, Chinese Academy of Sciences, Beijing 100080, People's Republic of China, [b]Institute of High Energy Physics, Chinese Academy of Sciences, Beijing 100049, People's Republic of China, [c]National Synchrotron Radiation Laboratory, University of Science and Technology of China, Hefei 230026, People's Republic of China, and [d]Graduate School of Science, Hokkaido University, Sapporo 0600810, Japan

‡ These authors contributed equally to this work.
§ Present address: SAIC-Frederick Inc., Basic Research Program, Argonne National Laboratory, Argonne, IL 60439, USA.

Correspondence e-mail: fanhf@cryst.iphy.ac.cn

Received 20 December 2005
Accepted 21 February 2006

The principle of dual-space phasing is used in dealing with protein SAD data. Four programs are involved in iterative dual-space fragment extension to improve automatic model building. *OASIS*-2004 is used to break the phase ambiguity intrinsic in the SAD experiment. In the initial cycle, discrimination of SAD phase doublets is performed by the direct method incorporating the known anomalous-scattering substructure. In subsequent cycles, discrimination is performed by the direct method incorporating both the known anomalous-scattering substructure and the partial protein structure obtained from model building in the preceding cycle. *DM* is used to improve direct-method phases *via* density modification. *RESOLVE* is used for initial model building and *ARP*/*wARP* is used to complete the structure. Case studies with three sets of difficult SAD data showed that the procedure is beneficial to high-throughput protein-structure determination and all of the four programs involved make their unique contribution to the process.

1. Introduction

Dual-space phasing (Weeks *et al.*, 1993; Sheldrick & Gould, 1995; Foadi *et al.*, 2000) has proved to be a powerful tool for the *ab initio* solution of protein structures with diffraction data at atomic resolution. For solving *de novo* protein structures with crystals that only diffract to lower resolution, the MAD (multi-wavelength anomalous diffraction) or SAD (single-wavelength anomalous diffraction) method is the first choice. The principle of dual-space phasing is also useful in dealing with SAD data at about 2 Å resolution, making the structure-determination process much more efficient and easy to automate. An iterative phasing/model-building procedure for processing SAD data has been proposed recently (Wang, Chen, Gu, Zheng & Fan, 2004). This dual-space procedure includes the initial direct-method phasing of SAD data, phase improvement *via* density modification, automatic model building and direct-method phasing of SAD data with feedback partial structure information. Advantages of the procedure in comparison with others in dealing with SAD data have been demonstrated by Watanabe *et al.* (2005) using a number of Cr $K\alpha$ sulfur SAD data. More than 20 sets of protein SAD data have been successfully tested with the dual-space phasing/model-building procedure. Table 1 summarizes some of the test data. Three of these were used as case studies in this paper, aiming at a deeper insight to the process.

Table 1
Summary of SAD data tested with the procedure described in this paper arranged in descending order of the expected Bijvoet ratio $\langle|\Delta F|\rangle/\langle F\rangle$.

Protein	Anomalous scatterers in the ASU	Wavelength (Å)	Expected $\langle|\Delta F|\rangle/\langle F\rangle$ (%)	Resolution limit (Å)	Residues in the ASU	Residues in the ASU found automatically	Reference
Trypsin	S (16)†	2.29 (Cr $K\alpha$)	4.2	2.02	223	220 (in 5 cycles)	Watanabe *et al.* (2005)
Lysozyme‡	S (16)†	2.29 (Cr $K\alpha$)	3.0	2.02	129	125 (in 7 cycles)	Watanabe *et al.* (2005)
CGL2612	Se (9)	2.29 (Cr $K\alpha$)	2.75	2.17	354	341 (in 2 cycles)	Itou *et al.* (2005)
Thaumatin	S (17)†	2.29 (Cr $K\alpha$)	2.5	2.02	207	203 (in 4 cycles)	Watanabe *et al.* (2005)
Rusticyanin	Cu (1)	1.38	2.36	2.10	154	140 (in 2 cycles)	Harvey *et al.* (1998)
PH1109	S (7)†	2.29 (Cr $K\alpha$)	2.27	2.17	144	144 (in 1 cycle)	Kitago *et al.* (2005)
Azurin‡	Cu (1)	0.97	1.44	1.90	129	116 (in 5 cycles)	Dodd *et al.* (1995)
Glucose isomerase	S (9)†	2.29 (Cr $K\alpha$)	1.2	2.17	388	381 (in 3 cycles)	Watanabe *et al.* (2005)
TT0570	S (20)†	2.29 (Cr $K\alpha$)	1.1	2.04	1206	1167 (in 3 cycles)	Watanabe *et al.* (2005)
Xylanase	S (6)†	1.74	0.69	1.63	303	302 (in 2 cycles)	Ramagopal *et al.* (2003)
Xylanase‡	S (6)†	1.49	0.56	1.75	303	299 (in 7 cycles)	Ramagopal *et al.* (2003)

† All anomalous scatterers found are treated as sulfur. ‡ Samples used for case studies in this paper.

2. The program *OASIS*-2004

OASIS-2004 (Wang, Chen, Gu, Zheng, Jiang & Fan, 2004; Wang, Chen, Gu, Zheng & Fan, 2004) is an updated version of *OASIS*. The latter has been included in the *CCP*4 suite (Collaborative Computational Project, Number 4, 1994) for experimental phasing of SAD/SIR data.

2.1. Initial phasing of SAD data

Most SAD phasing programs discriminate phase ambiguities using the known anomalous scattering substructure. They multiply the bimodal SAD phase distribution by the Sim distribution (Sim, 1959) to produce initial SAD phases. *OASIS* uses the product of the Cochran distribution (Cochran, 1955) and Sim distribution to discriminate SAD/SIR phase ambiguities. The process is outlined below.

The phase of an individual reflection is expressed as

$$\varphi_{\mathbf{h}} = \varphi''_{\mathbf{h}} \pm |\Delta\varphi_{\mathbf{h}}|. \tag{1}$$

In the SAD case $\varphi''_{\mathbf{h}}$ is the phase of $F''_{\mathbf{h}}$, which is contributed from the imaginary-part scattering of the anomalous scattering substructure,

$$F''_{\mathbf{h}} = i\sum_{j=1}^{N_{\rm ano}} \Delta f''_j \exp(i2\pi\mathbf{h}\cdot\mathbf{r}_{\rm ano}). \tag{2}$$

$|\Delta\varphi_{\mathbf{h}}|$ can be calculated from the known anomalous scattering substructure. The probability of the sign of $\Delta\varphi_{\mathbf{h}}$ being positive is given by

$$P_+(\Delta\varphi_{\mathbf{h}}) = \frac{1}{2} + \frac{1}{2}\tanh\left\{\sin|\Delta\varphi_{\mathbf{h}}|\left[\sum_{\mathbf{h}'} m_{\mathbf{h}'} m_{\mathbf{h}-\mathbf{h}'}\kappa_{\mathbf{h},\mathbf{h}'}\sin(\Phi'_3 + \Delta\varphi_{\mathbf{h}'\,\rm best} + \Delta\varphi_{\mathbf{h}-\mathbf{h}'\,\rm best}) + \chi\sin\delta_{\mathbf{h}}\right]\right\}, \tag{3}$$

with the associated best phase and figure of merit

$$\tanh(\Delta\varphi_{\mathbf{h}\,\rm best}) = 2\left[P_+(\Delta\varphi_{\mathbf{h}}) - \frac{1}{2}\right]\sin|\Delta\varphi_{\mathbf{h}}|/\cos\Delta\varphi_{\mathbf{h}}, \tag{4}$$

$$m_{\mathbf{h}} = \exp(-\sigma^2_{\mathbf{h}}/2)\left(\left\{2\left[P_+(\Delta\varphi_{\mathbf{h}}) - \frac{1}{2}\right]^2 + \frac{1}{2}\right\} \times (1-\cos 2\Delta\varphi_{\mathbf{h}}) + \cos 2\Delta\varphi_{\mathbf{h}}\right)^{1/2}. \tag{5}$$

The reader is referred to the paper by Fan & Gu (1985) for details. The above treatment renders the phase problem in the range 0–2π to a sign problem of making a choice between +1 and −1. The treatment also introduces the concept of lack-of-closure error into direct-method phasing. The practical advantage of this treatment has been examined by Wang, Chen, Gu, Zheng, Jiang, Fan *et al.* (2004).

2.2. Differences between *OASIS*-2004 and the preceding version

There are two major improvements in *OASIS*-2004. Firstly, the term related to the lack-of-closure error in (5) is expressed as

$$\sigma^2_{\mathbf{h}} = \frac{(n\sigma_{\Delta F_{\mathbf{h}}})^2}{2|F''_{\mathbf{h}}|^2}, \tag{6}$$

where n is a scaling factor, which previously had to be set manually for each particular set of SAD data. It is now automatically tuned in *OASIS*-2004. Details are given by Wang, Chen, Gu, Zheng, Jiang & Fan (2004).

Secondly, the term $\chi\sin\delta_{\mathbf{h}}$ in (3) was defined as being contributed from the anomalous scattering substructure. In *OASIS*-2004 the term is now defined in this way only for initial phasing in the first cycle. From the next cycle onwards, it is redefined as being contributed from the partial model obtained in the preceding cycle. The anomalous scattering substructure is kept fixed during the iteration. Reciprocal-space fragment extension is the most important function newly added to *OASIS*-2004. Details are given in Wang *et al.* (2004).

Source code, documentation and detailed examples of *OASIS*-2004 are available at http://cryst.iphy.ac.cn.

3. Phasing/model-building iteration

Fig. 1 shows a flow chart of the iterative phasing/model-building procedure. A set of SAD data is first processed in reciprocal space. *OASIS*-2004 is used to break the phase ambiguity intrinsic in SAD data, resulting in a set of 'best' phases and figures of merit for individual observed reflections. The output MTZ file is input to *DM* (Cowtan, 1994; Collaborative Computational Project, Number 4) for phase improvement *via* density modification. The output of *DM* is then passed on to automatic model building and structure refinement in real space. For this purpose, the program *RESOLVE* (build only; Terwilliger, 2003*a*,*b*) is used in the initial cycle(s), while the program *ARP*/*wARP* (Perrakis *et al.*, 1999) is used in subsequent cycles. The program *REFMAC* (Murshudov *et al.*, 1997) is called within *ARP*/*wARP* by default. Structure fragments and/or dummy atoms from model building are fed back to the program *OASIS*-2004 for reciprocal-space fragment extension (Wang, Chen, Gu, Zheng & Fan, 2004). In the present study, all programs were run in their default mode. No manual interventions were needed during the run.

It should be noticed that the program *RESOLVE* (Terwilliger, 2000) may be used instead of *DM* for density modification. Both programs usually produce good results. However, when one of them gets into trouble, it is recommended to try the other.

4. Data

The SAD data used in the case studies were from the proteins lysozyme, azurin and xylanase as summarized in Table 2. All the data sets were difficult to phase, as reported by Watanabe *et al.* (2005) for lysozyme, Wang, Chen, Gu, Zheng, Fan, Jiang *et al.* (2004) for azurin and Ramagopal *et al.* (2003) for xylanase. The sulfur-SAD data of xylanase collected with synchrotron radiation at $\lambda = 1.49$ Å has a very low expected Bijvoet ratio $\langle|\Delta F|\rangle/\langle F\rangle = 0.56\%$. To the knowledge of the authors, no successful phasing of this SAD data has been reported before.

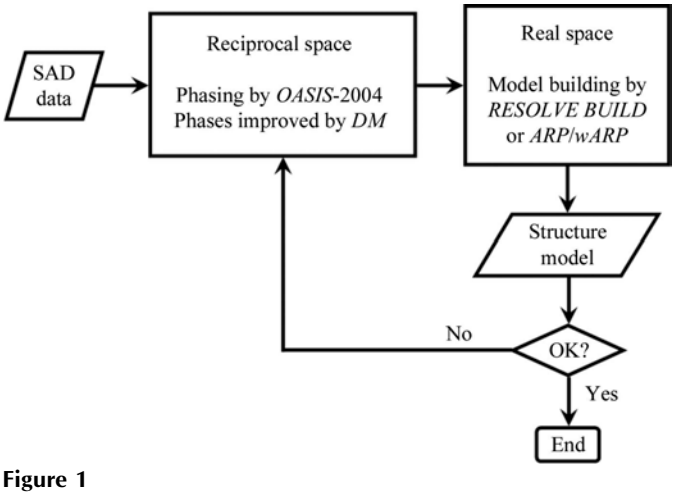

Figure 1
Flow chart of the iterative phasing/model-building procedure.

5. Results and discussion

The test results of lysozyme, azurin and xylanase are shown in Figs. 2, 3 and 4, respectively, of which parts (*a*) and (*b*) show the variation in unweighted averaged phase error during the phasing/model-building iteration and (*c*) shows the improvement of the electron-density map and the corresponding result of automatic model building according to protocol (i) described below. In the phasing/model-building iteration, each cycle consists of three steps: (i) direct-method phasing of SAD data by *OASIS*-2004 (Wang, Chen, Gu, Zheng, Jiang & Fan, 2004; Wang, Chen, Gu, Zheng & Fan, 2004), (ii) density-modification phase improvement by *DM* (Cowtan, 1994) and (iii) automatic model building by *RESOLVE* (build only; Terwilliger, 2003*a*,*b*) or *ARP*/*wARP* (Perrakis *et al.*, 1999). Three protocols of iteration have been tested: (i) *RESOLVE* (build only) is used for model building of cycle 0, while *ARP*/*wARP* is used for that of the rest, (ii) model building is performed as the same as (i), but *OASIS*-2004 is only used in the first few cycles and is then bypassed in subsequent cycles and (iii) model building is performed by *ARP*/*wARP* in all cycles. The results of protocols (i) and (ii) are shown as the cyan curve and black curves, respectively, in Figs. 2(*a*), 3(*a*) and 4(*a*). The results of protocol (iii) are shown in Figs. 2(*b*), 3(*b*) and 4(*b*). Ribbon models were plotted using *PyMOL* (DeLano, 2002). Electron-density maps were plotted using *O* (Jones *et al.*, 1991).

5.1. Lysozyme case

Fig. 2(*a*) shows that the dual-space phasing/model-building procedure is capable of solving the structure of lysozyme using the SAD data, since the unweighted averaged phase error fell from more than 60° to less than 40° within six cycles of iteration. In cycle 0, *OASIS*-2004 yielded an initial phase error of ∼64°, a fairly good value for initial phasing. *DM* brought it down to ∼57°. The electron-density map shown on the left of Fig. 2(*c*) reveals the essential features of the structure. *RESOLVE* (build only) raised the error to ∼70°, signifying not very successful model building. However, *RESOLVE* still gave correct and useful structure fragments, as shown at the top left of Fig. 2(*c*), which contain ∼55% of the total number of independent residues without side chains. In cycles 1–6, while the phase errors from different programs vary up and down as shown by the cyan curve in Fig. 2(*a*), the phase error resulting from the same program decreases continuously. Of the programs involved, *DM* is the one which always improved phases significantly in all cycles. From cycle 2 onwards, the program *OASIS*-2004 made phases worse than those from the previous run of *ARP*/*wARP*, increasing the average error by several degrees. Two tests have been performed to examine the necessity of *OASIS*-2004. Firstly, the program *OASIS*-2004 was bypassed from cycle 2 onwards. Phases from *ARP*/*wARP* in cycle 1 were directly input into *DM* in cycle 2. This resulted in the upper black curve in Fig. 2(*a*). It is seen that when bypassing *OASIS*-2004 the iteration was not successful. The reason is that while *OASIS*-2004 changes phases from *ARP*/*wARP* and increases their error, it helps phases to jump out of

a local minimum in *ARP*/*wARP*, enabling them to subsequently drop into a lower one, as shown by the cyan zigzag curve in Fig. 2(*a*). On the other hand, in cycle 5 *ARP*/*wARP* was capable for the first time of decreasing the phase error from the preceding run of *DM*. This signifies that the iteration is approaching the complete structure. At this point a second test was performed by bypassing *OASIS*-2004 from the next cycle. This gave a slightly better result as shown by the lower black curve in Fig. 2(*a*). This implies that when the phases are accurate enough for *DM* + *ARP*/*wARP* to approach the

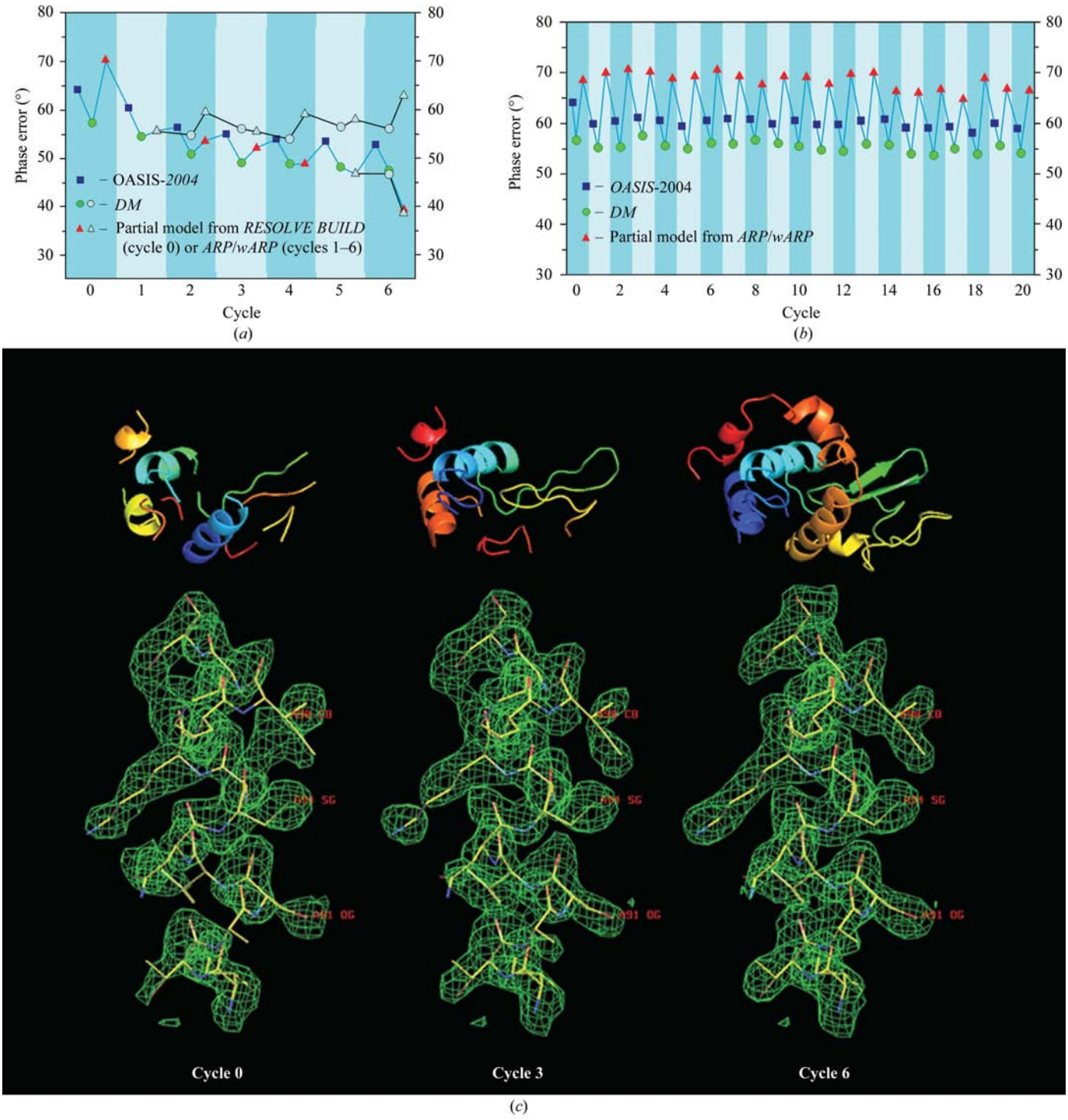

Figure 2
Results of phasing the Cr $K\alpha$ sulfur-SAD data of lysozyme. (*a*) Variation of the averaged phase error during the phasing/model-building iteration with *RESOLVE* (build only) for model building in cycle 0 and *ARP*/*wARP* in that of subsequent cycles. (*b*) Variation of the averaged phase error during the iteration with *ARP*/*wARP*for model building through out all cycles. (*c*) Improvement of the electron-density map (contoured at 1σ) and the corresponding automatic model building during the iteration according to protocol (i).

complete structure, *OASIS*-2004 is no longer necessary. For unknown protein structures it is difficult to decide where to start bypassing the program *OASIS*-2004. Hence, it is recommended to continue using it in all cycles. Fig. 2(*b*) shows the lysozyme result of protocol (iii), in which *ARP/wARP* is used throughout all cycles for model building. It is seen that in

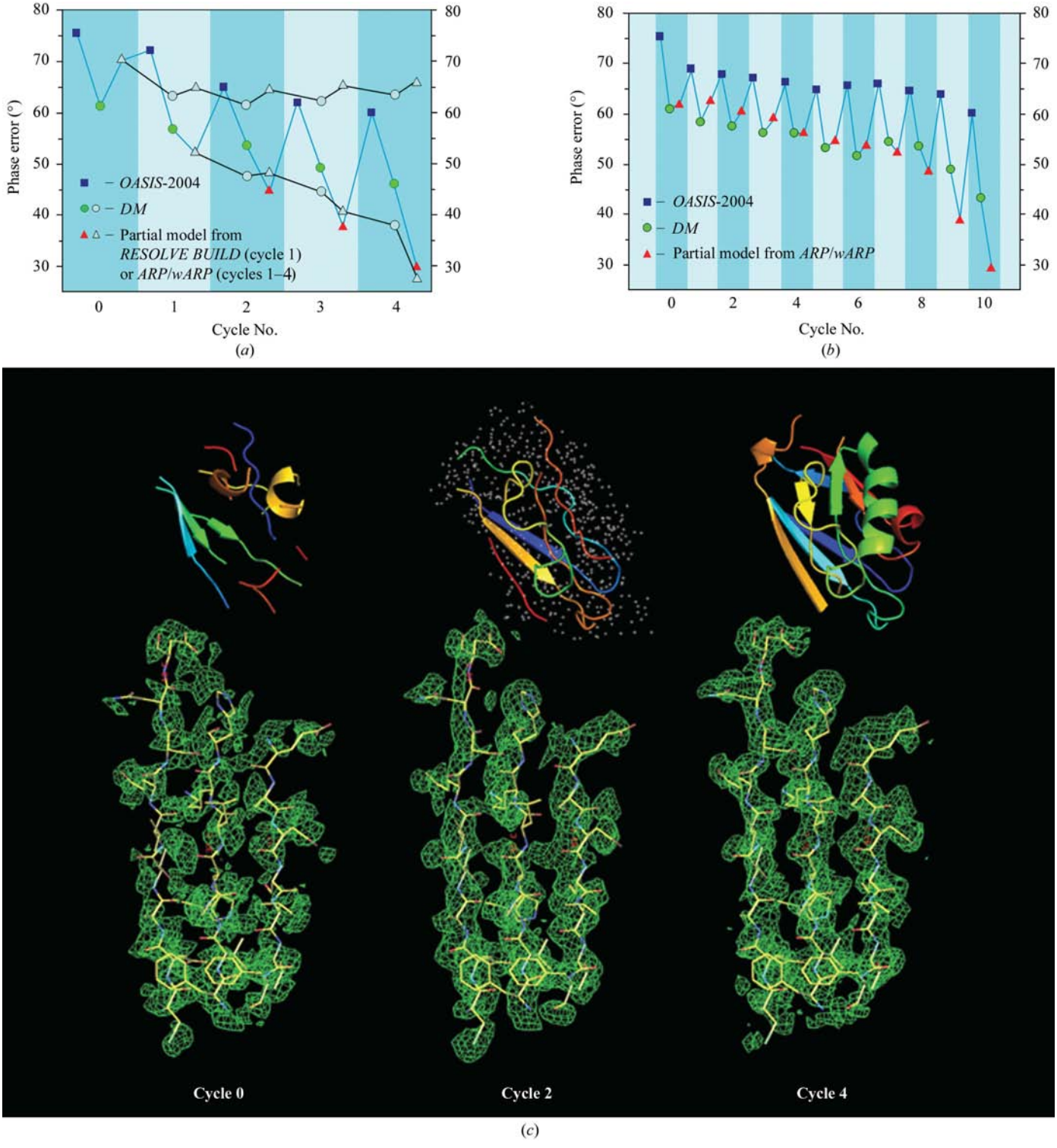

Figure 3
Results of phasing the synchrotron (0.97 Å) Cu-SAD data of azurin. (*a*) Variation of the averaged phase error during the phasing/model-building iteration with *RESOLVE* (build only) for model building in cycle 0 and *ARP/wARP* in subsequent cycles. (*b*) Variation of the averaged phase error during the iteration with *ARP/wARP* for model building throughout all cycles. (*c*) Improvement of the electron-density map (contoured at 1σ) and the corresponding automatic model building during the iteration according to protocol (i).

all 20 cycles *ARP/wARP* yielded the highest phase error, which varies from 65° to over 70° and is about 10° greater than that from the preceding run of *DM*. This means that the phasing/model-building iteration could not succeed without using *RESOLVE* to build the initial model. Fig. 2(*c*) shows the same portion of the *DM*-phased electron-density map and the corresponding result of automatic model building at different stages of iteration according to protocol (i). As is seen, the electron-density maps improved continuously and the model building improved dramatically. The last model, shown at the

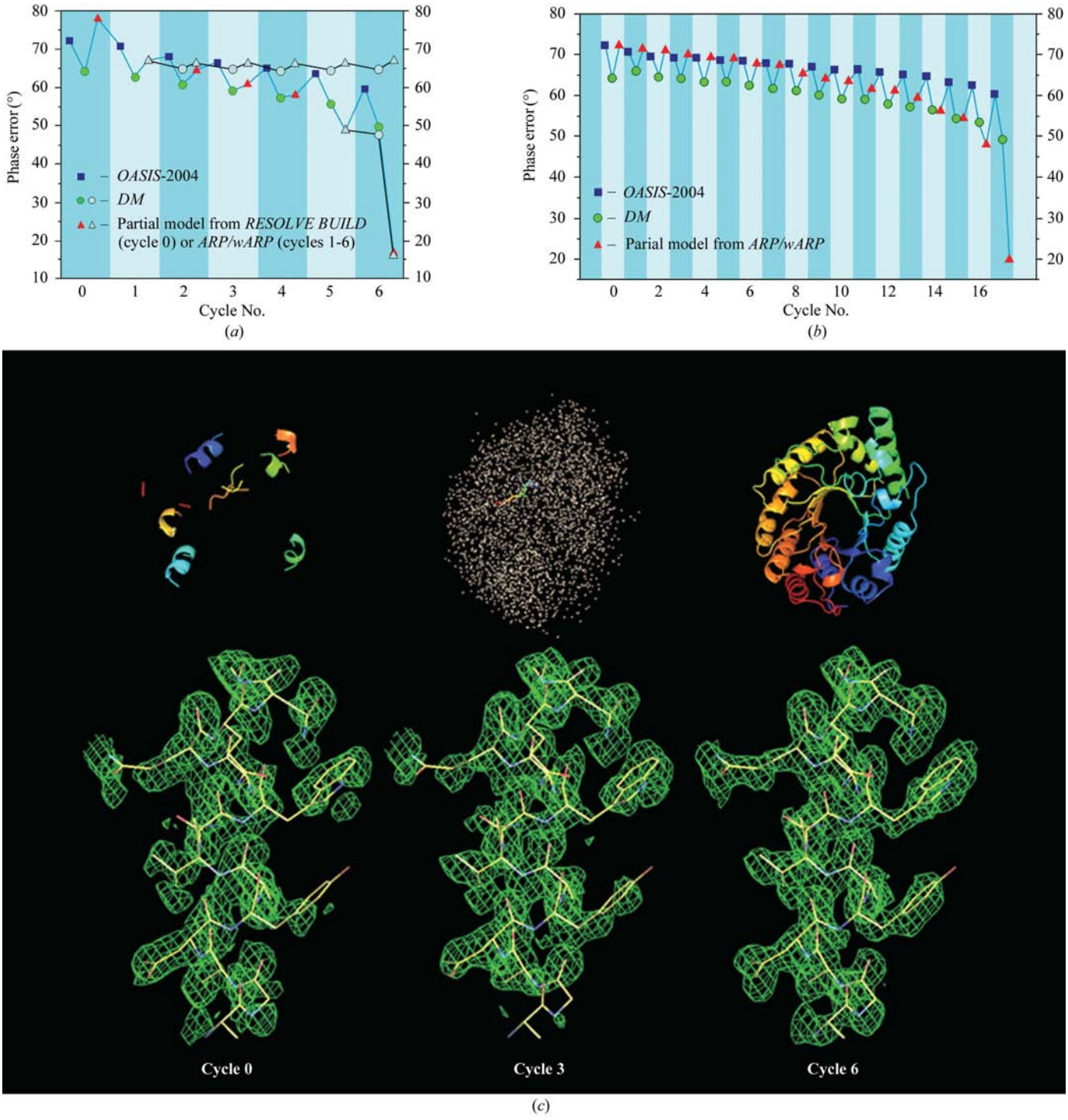

Figure 4
Results of phasing the synchrotron (1.49 Å) sulfur-SAD data of xylanase. (*a*) Variation of the averaged phase error during the phasing/model-building iteration with *RESOLVE* (build only) for model building in cycle 0 and *ARP*/*wARP* in subsequent cycles. (*b*) Variation of the averaged phase error during the iteration with *ARP*/*wARP* for model building throughout all cycles. (*c*) Improvement of the electron-density map (contoured at 1σ) and the corresponding automatic model building during the iteration according to protocol (i).

Table 2
Summary of samples used for case studies.

Protein	Lysozyme	Azurin	Xylanase
Space group	$P4_32_12$	$P4_122$	$P2_1$
Unit-cell parameters (Å, °)	a = 78.4, c = 37.0	a = 52.65, c = 100.63	a = 41.19, b = 67.18, c = 50.88, β = 113.5
No. of residues in the ASU	129	129	303
Resolution limit (Å)	2.02	1.9	1.75
X-ray source	Cr $K\alpha$ (rotating anode)	Synchrotron	Synchrotron
Wavelength (Å)	2.29	0.97	1.49
Anomalous scatterer†	S (16)	Cu (1)	S (6)
Expected $\langle\|\Delta F\|\rangle/\langle F\rangle$‡ (%)	3.0	1.44	0.56
Multiplicity	47.2	10.0	15.9
Reference	Watanabe *et al.* (2005)	Dodd *et al.* (1995)	Ramagopal *et al.* (2003)

† *SAPI* (Fan *et al.*, 1991) was used to find anomalous scatterers in azurin. *SHELXD* (Usón & Sheldrick, 1999) and *SOLVE* (Terwilliger & Berendzen, 1999) were used to locate and refine anomalous scatterers in lysozyme and xylanase. For these two proteins we did not distinguish chlorine or other heavy atoms from sulfur, the joint number of which is determined by *SHELXD* and *SOLVE*. ‡ Calculated according to the anomalous scatterers given in the previous row.

Table 3
Number of residues found automatically in each cycle of iteration.

(A) model built by *ARP/wARP*; (R) model built by *RESOLVE* (build only).

Protein (No. of residues in the ASU)	Lysozyme (129)	Azurin (129)	Xylanase (303)
No. of residues found (No. of residues docked into sequence)			
Cycle 0 (R)	71 (0)	58 (0)	62 (0)
Cycle 1 (A)	58 (0)	47 (0)	0 (0)†
Cycle 2 (A)	82 (0)	81 (41)	0 (0)†
Cycle 3 (A)	79 (48)	106 (97)	5 (0)
Cycle 4 (A)	93 (69)	116 (116)	15 (0)
Cycle 5 (A)	100 (67)		82 (0)
Cycle 6 (A)	125 (125)		299 (299)
Ratio of No. of residues found to No. of residues in the ASU (%)			
Start	55	45	21
End	97	90	99

† The model contains only dummy atoms.

upper right of Fig. 2(*c*), built in cycle 6 contains ∼97% of the total number of independent residues all docked into the sequence.

5.2. Azurin case

In the azurin case, the starting phase error from *OASIS*-2004 is about 76°, a not very good but still acceptable value. From the phase-error variation of azurin, shown as the cyan curve in Fig. 3(*a*), it is seen that the phasing/model-building iteration led to the solution of azurin in four cycles. It is confirmed by the upper black curve that *OASIS*-2004 is necessary in cycle 0 and cycle 1, since bypassing *OASIS*-2004 from cycle 1 led to failure of the iteration. We see again from the lower black curve that once *ARP*/*wARP* is able to decrease the phase error from the preceding run of *DM*, *OASIS*-2004 can be bypassed from the next cycle onward. In contrast to the lysozyme case, azurin could be solved without starting from a *RESOLVE*-built model, as is shown by Fig. 3(*b*). However, the cost is a doubling of the number of cycles of iteration. Fig. 3(*c*) shows the same portion of the *DM*-phased electron-density map and the corresponding result of automatic model building at different stages of iteration according to protocol (i). Again, we see that the electron-density maps improved continuously and the model building improved dramatically. The first model built in cycle 0 contains ∼45% of the total number of independent residues without side chains. The last model built in cycle 4 contains ∼90% of the total number of independent residues all docked into the sequence. The model in cycle 2 contains discrete dots in addition to ribbons. These are dummy atoms from *ARP*/*wARP*. While they do not carry any secondary-structure information of the protein, it is essential to include them in the partial model to be fed back to *OASIS*-2004 for reciprocal-space fragment extension. This will be discussed further in the next section.

5.3. Xylanase case

Fig. 4(*a*) is similar to Figs. 2(*a*) and 3(*a*), indicating that the structure of xylanase could be solved in six cycles of phasing/model-building iteration, as shown by the cyan curve. Again, it is seen that *OASIS*-2004 is inevitable in the early cycles (upper black curve). However, it can be bypassed after *ARP*/*wARP* has managed to lower the phase error from *DM* (lower black curve). Fig. 4(*b*) is similar to Fig. 3(*b*) but different to Fig. 2(*b*), *i.e.* the structure of xylanase could be solved *via* phasing/model-building iteration without using *RESOLVE*. However, the cost is unreasonably high: the number of cycles of iteration needed to be tripled. While the initial electron-density map of xylanase is not bad, as shown on the left of Fig. 4(*c*), the first model in cycle 0 shown at the upper left of Fig. 4(*c*) contains only ∼21% of the total number of independent residues without side chains. Nevertheless, six cycles of phasing/model-building iteration led to the model shown at the upper right of Fig. 4(*c*), which contains ∼99% of the total number of independent residues all docked into the sequence. Xylanase SAD phasing at 1.49 Å may be the most difficult case so far published. A detailed comparison of the iteration process between lysozyme, azurin and xylanase is given in Table 3. A significant feature of xylanase is that from cycle 1 to cycle 5 *ARP*/*wARP* produced no or very poor secondary structures. Models from *ARP*/*wARP* within these cycles consist of only or mainly dummy atoms and no residues in the model are docked into the sequence. However, a nearly complete model suddenly appeared in cycle 6. This implies that while dummy atoms might not be useful in the conventional fragment-extension process, they are very important in dual-space fragment extension involving the direct method in *OASIS*-2004. The reason is that according to the probability formula (3), even a set of dummy atoms will significantly affect the direct-method phasing *via* the term $\chi \sin\delta_{\mathbf{h}}$. When dummy atoms are roughly distributed within the protein region in the unit cell, the phases of low-resolution strong reflections will be

improved, leading to significantly better electron-density maps.

6. Concluding remarks

The phasing of xylanase SAD data at a wavelength of 1.49 Å had been an impossible task for existing methods, as described by Ramagopal *et al.* (2003). The successful phasing of this SAD data by the dual-space iteration described in the present paper pushed the practically usable Bijvoet ratio down to a new lower limit of 0.56%. Dual-space fragment extension is a powerful tool for automatic structure determination of proteins using SAD data at ∼2 Å resolution or better. The procedure can dramatically enhance the power of automatic model building and hence it is important to the high-throughput determination of protein structures. Further improvement of the method will be to extend the applicability to SAD data at lower resolution, say ∼3 Å.

HFF would like to thank Drs S. S. Hasnain and Z. Dauter for kindly making available the SAD data of azurin and xylanase, respectively. This work is supported by the Innovation Project of the Chinese Academy of Sciences and the 973 Project (Grant No. 2002CB713801) of the Ministry of Science and Technology of China.

References

Cochran, W. (1955). *Acta Cryst.* **8**, 473–478.
Collaborative Computational Project, Number 4 (1994). *Acta Cryst.* D**50**, 760–763.
Cowtan, K. (1994). *Jnt CCP4/ESF–EACBM Newsl. Protein Crystallogr.* **31**, 34–38.
DeLano, W. L. (2002). *The PyMOL Molecular Graphics System.* DeLano Scientific, San Carlos, CA, USA.
Dodd, F., Hasnain, S. S., Abraham, Z. H., Eady, R. R. & Smith, B. E. (1995). *Acta Cryst.* D**51**, 1052–1064.
Fan, H.-F. & Gu, Y.-X. (1985). *Acta Cryst.* A**41**, 280–284.
Fan, H. F., Yao, J.-X., Zheng, C.-D., Gu, Y.-X. & Qian, J.-Z. (1991). *SAPI91. A Computer Program for Automatic Solution of Crystal Structures from X-ray Diffraction Data.* Institute of Physics, Chinese Academy of Sciences, Beijing, People's Republic of China.
Foadi, J., Woolfson, M. M., Dodson, E. J., Wilson, K. S., Yao, J.-X. & Zheng, C.-D. (2000). *Acta Cryst.* D**56**, 1137–1147.
Harvey, I., Hao, Q., Duke, E. M. H., Ingledew, W. J. & Hasnain, S. S. (1998). *Acta Cryst.* D**54**, 629–635.
Itou, H., Okada, U., Suzuki, H., Yao, M., Wachi, M., Watanabe, N. & Tanaka, I. (2005). *J. Biol. Chem.* **280**, 38711–38719.
Jones, T. A., Zou, J. Y., Cowan, S. W. & Kjeldgaard, M. (1991). *Acta Cryst.* A**47**, 110–119.
Kitago, Y., Watanabe, N. & Tanaka, I. (2005). *Acta Cryst.* D**61**, 1013–1021.
Murshudov, G. N., Vagin, A. A. & Dodson, E. J. (1997). *Acta Cryst.* D**53**, 240–253.
Perrakis, A., Morris, R. & Lamzin, V. S. (1999). *Nature Struct. Biol.* **6**, 458–463.
Ramagopal, U. A., Dauter, M. & Dauter, Z. (2003). *Acta Cryst.* D**59**, 1020–1027.
Sheldrick, G. M. & Gould, R. O. (1995). *Acta Cryst.* B**51**, 423–431.
Sim, G. A. (1959). *Acta Cryst.* **12**, 813–815.
Terwilliger, T. C. (2000). *Acta Cryst.* D**56**, 965–972.
Terwilliger, T. C. (2003*a*). *Acta Cryst.* D**59**, 38–44.
Terwilliger, T. C. (2003*b*). *Acta Cryst.* D**59**, 45–49.
Terwilliger, T. C. & Berendzen, J. (1999). *Acta Cryst.* D**55**, 849–861.
Usón, I. & Sheldrick, G. M. (1999). *Curr. Opin. Struct. Biol.* **9**, 643–648.
Wang, J.-W., Chen, J.-R., Gu, Y.-X., Zheng, C.-D. & Fan, H.-F. (2004). *Acta Cryst.* D**60**, 1991–1996.
Wang, J.-W., Chen, J.-R., Gu, Y.-X., Zheng, C.-D., Jiang, F. & Fan, H.-F. (2004). *Acta Cryst.* D**60**, 1987–1990.
Wang, J.-W., Chen, J. R., Gu, Y.-X., Zheng, C.-D., Jiang, F., Fan, H.-F., Terwilliger, T. C. & Hao, Q. (2004). *Acta Cryst.* D**60**, 1244–1253.
Watanabe, N., Kitago, Y., Tanaka, I., Wang, J.-W., Gu, Y.-X., Zheng, C.-D. & Fan, H.-F. (2005). *Acta Cryst.* D**61**, 1533–1540.
Weeks, C. M., DeTitta, G. T., Miller, R. & Hauptman, H. A. (1993). *Acta Cryst.* D**49**, 179–181.